



ISSN: 0975-833X

Available online at <http://www.journalcra.com>

International Journal of Current Research
Vol. 12, Issue, 01, pp.9235-9248, January, 2020

DOI: <https://doi.org/10.24941/ijcr.37048.01.2020>

INTERNATIONAL JOURNAL
OF CURRENT RESEARCH

RESEARCH ARTICLE

MODELING, DESIGN AND ANALYSIS OF A TRANSMISSION SHAFT OF A SOLAR HAMMER MILL

Sidi Bouhamady^{1,*}, Mouhamadou THIAM², Hoavo Hova³, Mohamed Lemine Hamza⁴ and Ibrahima Ly⁵

¹Laboratoire d'Energétique Appliquée, Ecole Supérieure Polytechnique de Dakar, BP 5085 Sénégal

²Laboratoire d'Energies Renouvelables, Ecole Supérieure Polytechnique de Dakar, BP 5085 Sénégal

³Laboratoire Matériaux, Energie Renouvelable et Environnement, Université de Kara, BP 404 Kara, Togo

⁴Département Energie et Propulsion, Académie Navale, BP 880, Nouadhibou, Mauritanie

⁵Département Electromécanique, Ecole Polytechnique de Thiès, BP 10, Sénégal

ARTICLE INFO

Article History:

Received 24th October, 2019

Received in revised form

18th November, 2019

Accepted 29th December, 2019

Published online 30th January, 2020

Key Words:

Solar hammer mill, Rural Area,
Modeling and Design,
Dimensioned, ASME Code,
Finite Element Analysis.

ABSTRACT

The objective of this article is to make the design and the validation of a solar mill for rural use. Based on the operating principle of the solar hammer mill, a transmission tree was being created, modeled and dimensioned. The tree behavior is obtained by analyzing its operation in all cases of possible load. The design and dimensioning were carried out based on analytical and empirical equations such as the ASME code. Five diameters (8 mm, 15 mm, 25 mm, 35 mm and 50 mm) were evaluated according to different types of materials. The evaluation of the type of tree materials has optimized its weight from 40% to 70%. CATIA logical via the method by Finite Element Analysis was used to construct the three-dimensional model and realize the dynamic simulation of the mechanism. The optimal choice of diameter 25 mm of material 4 CD 16 was made because of a good compromise of resistance-weight. These results indicate that the maximum equivalent von Mises stress is of the order 39.4 MPa with a maximum value of the static deformation is of the order of 1.25×10^{-2} mm.

Copyright © 2020, Sidi BOUHAMADY et al. This is an open access article distributed under the Creative Commons Attribution License, which permits unrestricted use, distribution, and reproduction in any medium, provided the original work is properly cited.

Citation: Sidi BOUHAMADY, Mouhamadou THIAM, Hoavo Hova, Mohamed Lemine Hamza and Ibrahima Ly. 2020. "Modeling, Design and Analysis of a Transmission Shaft of a Solar Hammer Mill", *International Journal of Current Research*, 12, (01), 9235-9248.

INTRODUCTION

The transmission shaft in a solar hammer mill is an essential mechanical member in the machine. It transmits motion and door hammers, which are in their turn, crush millet grains to accomplish the required function of the machine. Initially, the model was created using the database available of engine such as power to be transmitted and frictional forces millet grains on the hammers. The tree is subjected to two simultaneous stresses: the torque created by the drive motor and the bending moment due to friction forces hammers. Following the service conditions trees, materials must have high strength characteristics. The trees design process is usually limited to conventional algorithms that involve the use of analytical and empirical equations. Several design standards (Shigley, 1989), (Standard, 1985), (Spotts, 1991) such as the American National Standards Institute (ANSI) and the American Society of Mechanical Engineers (ASME) can be used as a guide for designer's trees. Nowadays, these calculations can be combined with simulations performed by CAD software, based on the method of analysis by finite element (FEA) and other optimization methods (Ranganath, 2004). In the case of design of trees for a hammer mill it is necessary to propose a shaft design bespoke extreme conditions that is to say in regime where the machine is a very solicited. This document presents the important aspects of a practical methodology applied to the design, sizing and analysis of the behavior of a tree of a solar hammer mill, the following steps were undertaken: First, identification of different operating diets of the machine, choice the design dimensions, Elaboration effort diagrams to determine the equivalent moment of the critical section the tree, application of ASME Code to find the diameter value for five different materials, verification of different diameters evaluated by the ASME code by a method of Finite element analysis in the CATIA environment to determine at any point of the geometry of the shaft the equivalent Von Mises stress, displacement and static deformation while making optimum choice of material guarantees a good compromise of resistance-weight.

*Corresponding author: Sidi Bouhamady,

Laboratoire d'Energétique Appliquée, Ecole Supérieure Polytechnique de Dakar, BP 5085 Sénégal.

1. Study the current system: The solar mill present, created by the Spanish inventor Syphili which the company called Alternativas C M R, S. L. (GTZ, Février 2004.). The principle of mill is similar off at hammer mill. The technical characteristics of model are listed in Table 1 and 2.

Table 1. Technical specifications of the mill Voltage V

	Power kW	Flow kg/h	Starting system
24V, continuous current	1,5	150 kg/h	rhéostat

Table 2. Specifications with autonomy of 2 hours / day

PV generator	power Wp	Battery	Controller / shedder
24V, Continuouscurrent	600	100Ah 10 Batteries	100kg

This moulin was Studied by LER (Laboratoire d'Énergie Renouvelable) of Ecole Supérieure Polytechnique de Dakar to provetheir performance. The Montegrisol model is facing some technical problems in its current state. These problems are related firstly to the protection mechanism of the mechanical parts and the quality of the final version. The machine drive motor is not protected nor standardized. Indeed the motor shaft has been extended by another welded on which the hammer holder.



Figure 1. Solar mill study

This solution induces several risks, firstly, a simple blockage may cause the motor loss is the system drive member, and therefore the cost of the system becomes high, the system balancing is no longer ensured due to the added axle and welding result in poor quality of the grind, In case of a strong imbalance, the rotating part (hammers) can affect the fixed part (sieves). These problems cause the reduction of the lifetime of the system.

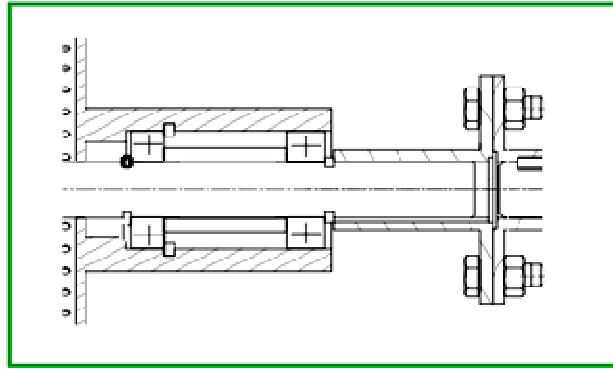


Figure 2. Flange coupling

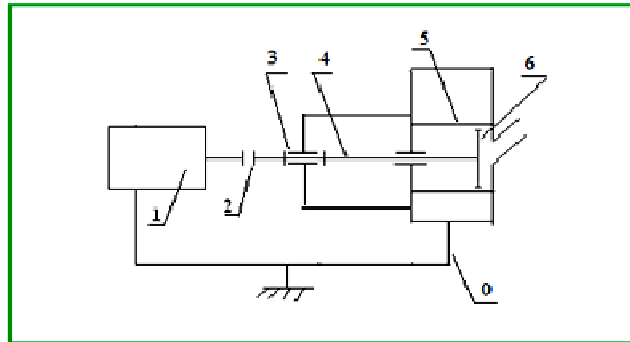


Figure 3. Kinematic diagram of the machine to achieving

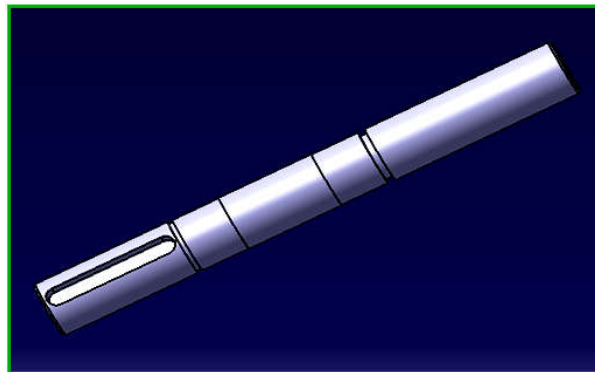


Figure 4. Geometric model of the shaft

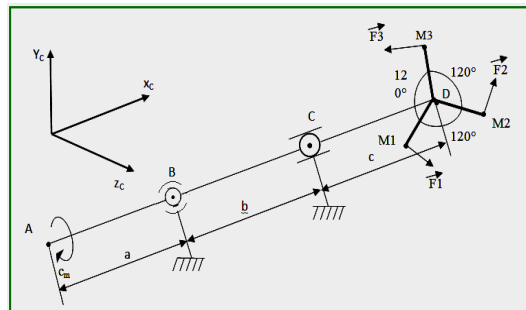


Figure 5. Mechanism modeling in normal regime

These mills are operated in rural areas of Senegal where there is a shortage of spare parts and breach of skilled works hand hence the need to provide a secure system while thinking to socio-economic realities of populations these areas. Several solutions have been proposed to protect the engine and ensure the stability and quality of milling system. The first is to establish a flange coupling (Figure 2) connecting the axis of the driving motor and a shaft on which the hammers are fixed. This solution is accompanied by a rotation guide system of this shaft in order to ensure better stability and balancing where a milling quality

mechanism. The choice of the above solutions were made taking into account factors related to the proper functioning of the system studied (security) and the available manufacturing capabilities

1.1. Description and modeling of the proposed mechanism: The kinematic diagram of Figure 3 shows a millet mill consisting of an asynchronous motor (1) of 1,5kW, this causes the transmission shaft (4) grace of a resilient coupling (2), and guided in rotation by bearings has a row of balls (3). The rotation of the drive shaft causes the hammers (6) which are secured thereto, the latter are within a sieve (5) which contains the grains to grind coming from the feed hopper and which are overwritten on one another under the percussion effect, until they are sprayed through the sieve mesh, the mechanism based on the frame (0). The main objective of this work is to dimension and analyze the mechanical behavior of the drive shaft 4 of the mechanism (Figure 4).

1.1.1. Modeling of the mechanism: The mechanism shown in Figure 5 mainly consists of a drive shaft, rotated by an elastic coupling at point A, via an asynchronous electric motor, and guided in rotation by ball bearings, (Modeled by a annular linear link of axis (C, x), patella link of center B), At the end of the shaft to the point M1 we have the resisting force on the hammers.

Hypotheses: All weights rotating parts are neglected.

•All parts are rigid and dimensionally stable and all links are perfect.

The analysis of the system has identified two possible models following its workings regime: model in regime established – permanent and model said abnormal – blocking.

1.1.1.1. Modelization in regime established – permanent: The mechanism diet is established when the angular speed of the drive motor is constant, in other words:

$$\frac{d\Omega}{dt} = 0 \quad (1)$$

In this regime the three hammers are subject to friction forces, with grains of millet, than we designated in Figure 5 by F1 F2, F3 at points M1, M2, M3. The dynamic general equation reduces to:

$$J \times \frac{d\Omega}{dt} = Cm - Cr = 0 \Rightarrow Cm = C \quad (2)$$

Calculation the effort F crushing the grains in normal regime - permanent:

Equation 3 gives the resistant torque:

$$Cr = F_1 \times \frac{dm}{2} + F_2 \times \frac{dm}{2} + F_3 \times \frac{dm}{2} \quad (3)$$

The grains are evenly distributed:

$$F_1 = F_2 = F_3 = F \quad (4)$$

Equation 3 becomes:

$$Cr = 3 \times \frac{dm}{2} \times F \quad (5)$$

From Equation 3 and 5:

$$F = \frac{2}{3} \times \frac{Cm}{dm} \quad (6)$$

Equation 7 gives the motor torque:

$$Cm = \frac{Pm}{\Omega} = \frac{1,5 \times 1000 \times 60}{2\pi \times 2850} = 5,02 \text{ N.m} \quad (7)$$

Equation 6 becomes:

$$F = \frac{2}{3} \times \frac{Cm}{dm} = 41,14 \text{ N} \quad (8)$$

1.1.1.1. Modelization in regime abnormal – blocking: The operation in abnormal regime where blocking consists to stuck one of the hammers in full operation while the others suffer no effort. In this regime, we model the wedging force by any force, which will be broken down in Figure 6 by a tangential force and normal force on the hammer.

Calculation the effort F crushing the grains in abnormal regime - blocking: In blocking regime, the crushing force F is calculated by the formula 9:

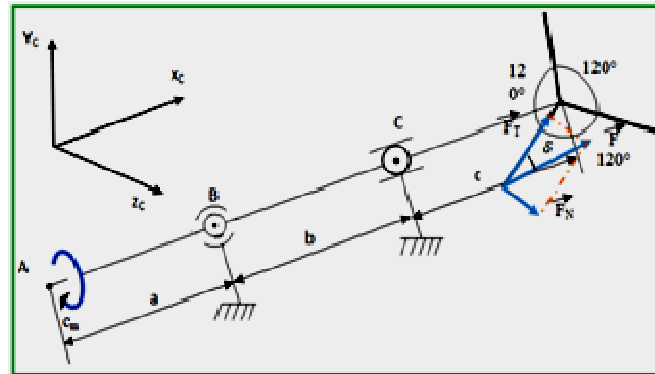
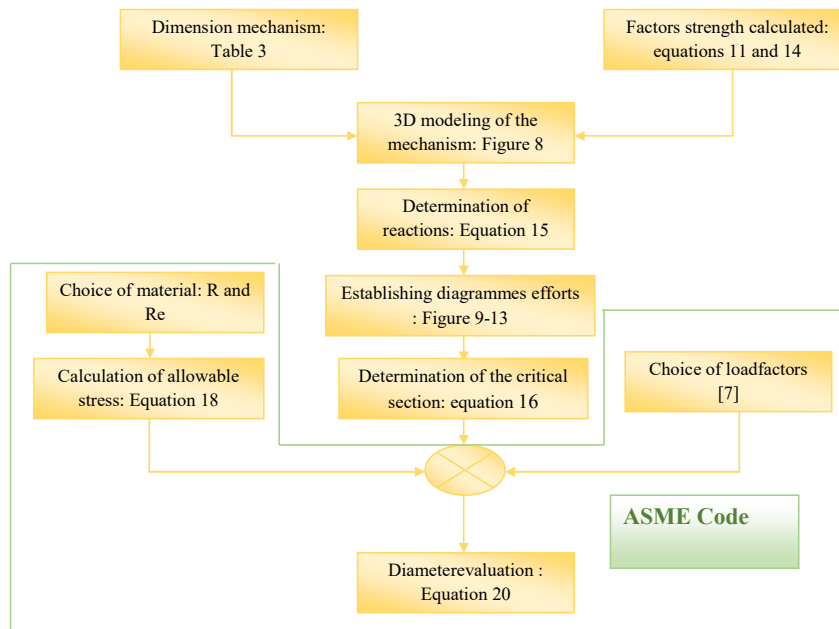


Figure 6. Mechanism modeling in abnormal regime



$$F = \sqrt{F_T^2 + F_N^2} \tag{9}$$

The blocking resistance torque is given by equation 10:

$$Cr = F_T \times \frac{dm}{2} \tag{10}$$

In blocking regime, the engine develops its maximum power to overcome the resisting torque. This power is estimated to be twice the rated power. The corresponding torque is determined by:

$$C_{max} = \frac{P_{max}}{\Omega} = \frac{2 \times 1,5 \times 1000 \times 60}{2\pi \times 2850} = 10,04 \text{ N.m} \tag{11}$$

At from Equation 10 and 11 the tangential component is given by:

$$F_T = \frac{2 \times C_{max}}{dm} \Rightarrow F_T = 164,6 \text{ N} \tag{12}$$

The normal component is given by:

$$F_N = \frac{F_T}{\tan \delta} \Rightarrow F_N = 417,83 \text{ N} \quad (13)$$

δ : friction angle, called talus angle of millet.(A.Gueye, juillet 1996) [6]

This angle is generally between 15° and 28° , we fixed a mean value $\delta = 21.5^\circ$

$$F = \sqrt{F_T^2 + F_N^2} = 418,02 \text{ N} \quad (14)$$

The goal to study the modeling of the proposed system in two cases of operation is to identify in what case of operating the system is very solicited.

The results show that in the abnormal operation, the effort is of 418.02 N, compared to 41.41 N in normal operation. Which leads to take into account the stresses in regime abnormal system for a credible dimensioning of the system, thereby increasing the lifetime of these components.

1.1.Sizing of the tree: The tree (AD) is subject to two simultaneous stresses: The torsion torque along its entire length created by the drive motor and the bending moment due to the friction forces hammers on the grains to grind and the reactions of the supports figure 7 shows the schematic flow diagram of the steps of the model to calculate the diameter of the shaft.

a) **3D Schematic:** The table 3, figure 8 gives the dimensions and 3D model for new machine, respectively

a) **Determination of the binding reactions**

$$\begin{aligned} &\{T(\text{Bati} \rightarrow 1)\} + \{T(\text{Bati} \rightarrow 1)\} + \{T(\text{Moteur} \rightarrow 1)\} + \\ &\{T(\text{Marteau} \rightarrow 1)\} = \{0\} \end{aligned} \quad (15)$$

$$\{T(\text{bati} \rightarrow 1)\} = \begin{Bmatrix} 0 & 0 \\ Y_C & 0 \\ Z_C & 0 \end{Bmatrix}_{C,R}$$

$$\{T(\text{Bati} \rightarrow 1)\} = \begin{Bmatrix} X_B & 0 \\ Y_B & 0 \\ Z_B & 0 \end{Bmatrix}_{B,R}$$

$$\{T(\text{Moteur} \rightarrow 1)\} = \begin{Bmatrix} 0 & -C_{\max} \\ 0 & 0 \\ 0 & 0 \end{Bmatrix}_{A,R}$$

Distances	AB	BC	BD
(mm)	40	40	160

The resolution of the system involves determining the mechanical actions in points B and C of the bearings, The Fundamental Principle of Static (FPS) on the drive shaft in the base $(A, \vec{x}, \vec{y}, \vec{z})$ reads:

$$\{T(\text{Marteau} \rightarrow 1)\} = \begin{Bmatrix} 0 & 0 \\ F * \sin(30 - \delta) & 0 \\ -F * \cos(30 - \delta) & 0 \end{Bmatrix}_{M,R}$$

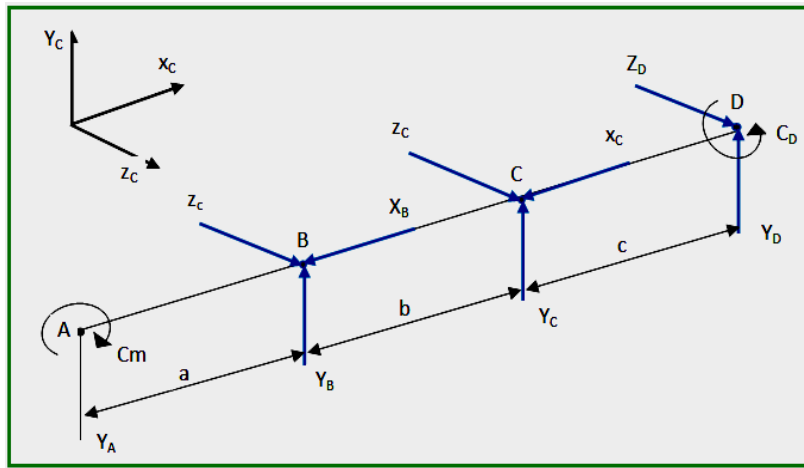


Figure 8. 3D Modeling System

$$\{T(\text{Marteau} \rightarrow 1)\} = \left\{ \begin{array}{cc} 0 & \sin \delta * \frac{dm}{2} * F \\ F * \sin(30 - \delta) & 0 \\ -F * \cos(30 - \delta) & 0 \end{array} \right\}_{D,R}$$

By bringing all the torques at the point B and applying, the FPS is obtained \Rightarrow

Load case (s)	Nodes	Abscisse x (mm)	Fz (N)	Fz (N)	Mz (N.mm)
	1	0	0	0	0
	2	40	-1240.3	-1240.3	0
	3	80	1653.84	1653.84	0
	4	200	-413.42	-413.42	0

Link (s) node (s)	Node 1
	housing

$$\left\{ \begin{array}{l} X_B = 0 \\ Y_B = \left(1 - \frac{BD}{BC}\right) * \sin(30 - \delta) * F \\ Z_B = \left(1 - \frac{BD}{BC}\right) * \cos(30 - \delta) * F \\ Y_C = -\frac{BD}{BC} * \sin(30 - \delta) * F \\ Z_C = \frac{BD}{BC} * \cos(30 - \delta) * F \end{array} \right.$$

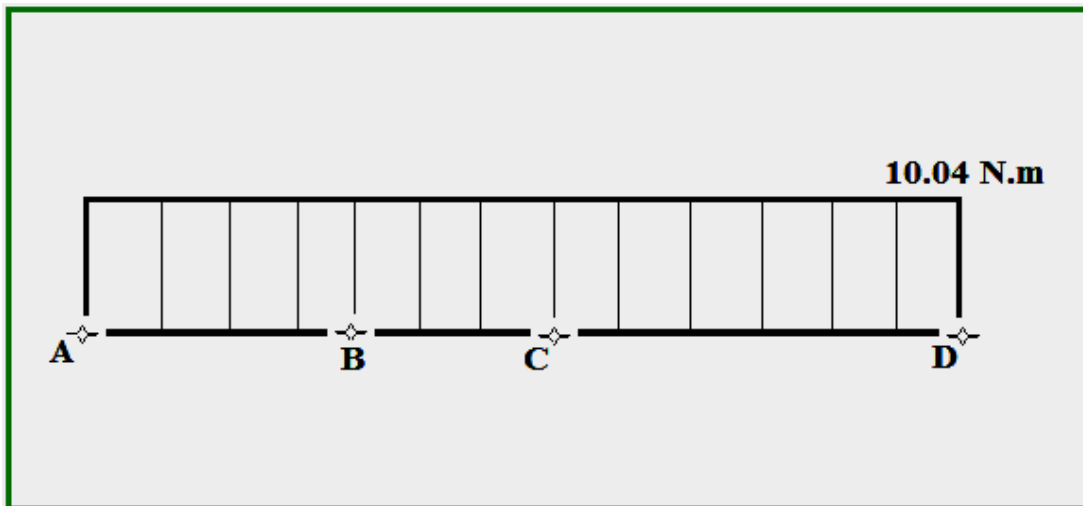


Figure 9. Diagram of the torsional moment distribution

Intérieurs efforts	Nodes	Shear force Ty (N)	Bending moment Mz (N.m)
	1 to 2	0.12	11.2 to 6.40
	2 to 3	1240.42	6.40 to 49610.4
	3 to 4	-413.42	-49610.40 to 0

Intérieurs efforts	Nodes	Shear force Ty (N)	Bending moment Mfz (N.mm)
	1 to 2	-368,98	-14680 to 79,20
	2 to 3	-183,63	79,20 to 7424,40
	3 to 4	61,87	7424,4 to 0

Tableau 5. Données obtenus (A,x,y)

Load case (s)	Nodes	Abscisse x (mm)	Fz (N)	Fz (N)	Mz (N.mm)
	1	0	0	0	0
	2	40	-1240.3	-1240.3	0
	3	80	1653.84	1653.84	0
	4	200	-413.42	-413.42	0

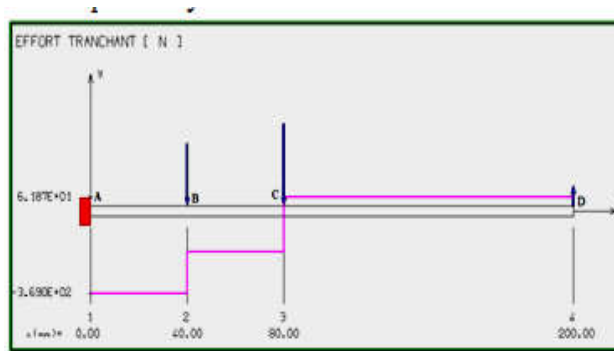


Figure 10. Cutting efforts Ty

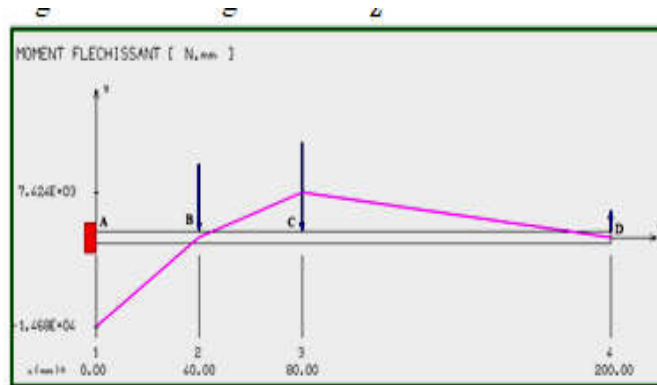


Figure 11. Moment bending diagram M_z :

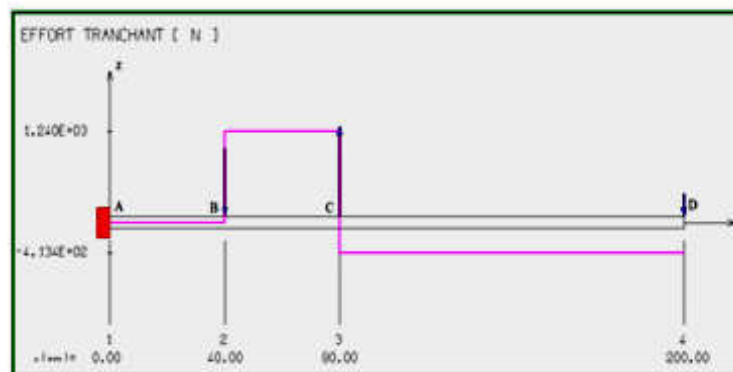


Figure 12. Diagram of cutting efforts Tz

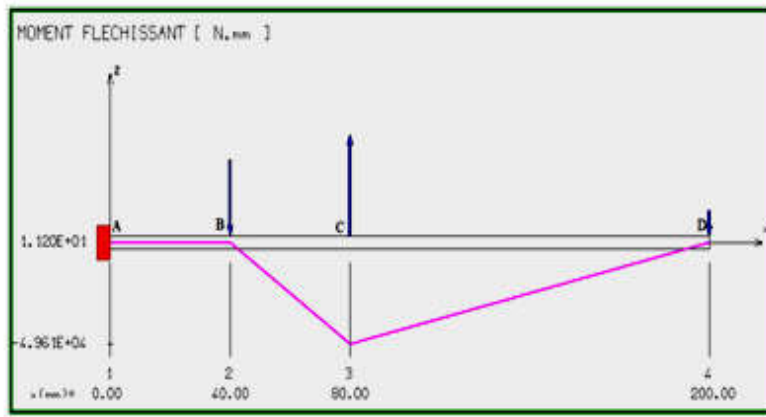


Figure 13. Moment bending diagram My

Table 8-diameter evaluated results.

Material	Mechanical characteristics (Re, R)	Constant b	Maximum allowable stress [σ]	Load Factors (Cm,Ct)	maximum bending moment in C	torsion moment	calculated diameter
steel S 235	(235, 340)	0,75	31,725	(1,5 ; 1)	50,2	10,04	37,6
steel S 335	(335, 490)	0,75	45,225	(1,5 ; 1)	50,2	10,04	33,4
42 CD 4	(700, 880)	0,75	94,5	(1,5 ; 1)	50,2	10,04	22,8
34 Cr Mo 4	(800, 500)	0,75	108	(1,5 ; 1)	50,2	10,04	13,1
36 Ni Cr Mo 16	(1000, 800)	0,75	135	(1,5 ; 1)	50,2	10,04	7,2

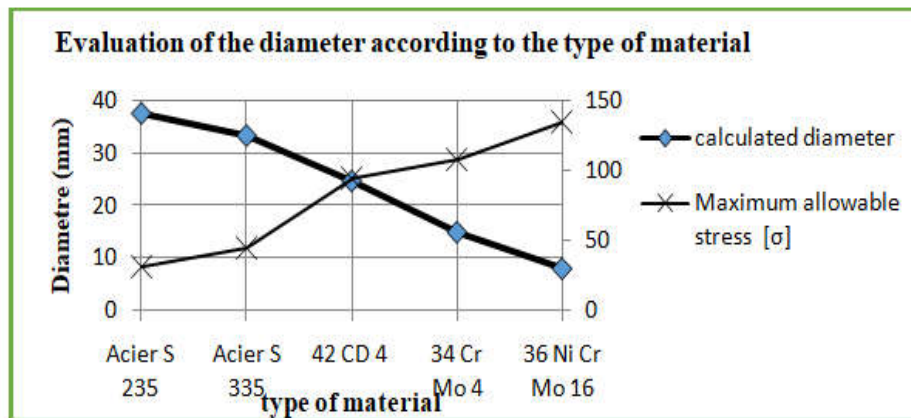


Figure 14. Evaluation of the diameter according to the type of material

Tableau 9. Simulation result

Material	Mechanical characteristics (Re, R)	safety factor	Allowable stress [σ]	calculated diameter	Equivalent stress Von Mises	Maximum static deformation	standard diameter
steel S 235	(235, 340)	3	78,33	37,6	22,35	Negligible	50
steel S 335	(335, 490)	3	111,66	33,4	24,66	Negligible	35
42 CD 4	(700, 880)	3	233,3	20,8	39,94	0,0125	25
34 Cr Mo 4	(800, 500)	3	266,66	13,1	66,27	Rupture	15
36 Ni Cr Mo 16	(1000, 800)	3	333,33	7,2	97,87	Rupture	8

Mechanical characteristics	Valeurs
elastic modulus E (MPa)	2 E+05
Poisson coefficient ν	0.32
shear modulus G (MPa)	7.57 E+05
density ρ (kg / m ³)	7500
Elasticity limit Re (MPa)	700

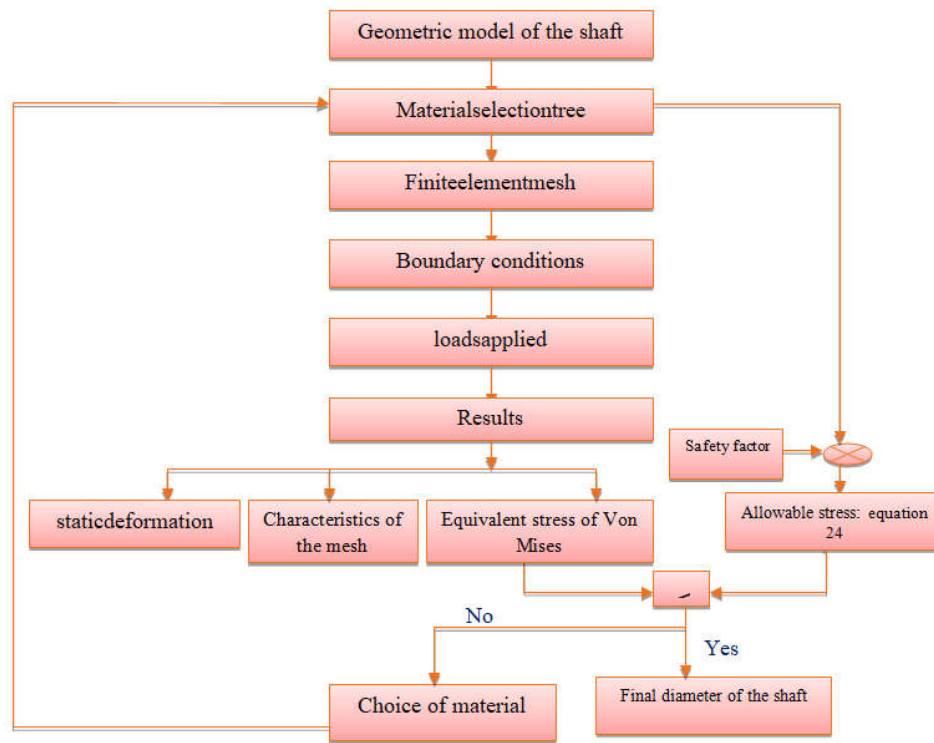


Figure 15. Diagram of the steps for the method FEA

Table 11. Loads applied

Loads applied	corresponding value
bearing effort (red)	$X_B = 0N; Y_B = -18535N; Z_B = -12403N;$
bending force of hammers on the shaft	$X_C = 0N; Y_C = -2475N; Z_C = 165384N$
Torque drive motor	$Y_D = 61,78N; Z_D = -413,4N;$ $C_D = 3,04N.m$

$$\Rightarrow \begin{cases} X_B = 0 \\ Y_B = -18535 \text{ N} \\ Z_B = -12403 \text{ N} \\ Y_C = -2475 \text{ N} \\ Z_C = 165384 \text{ N} \end{cases}$$

a) Determination of the moments diagrams

This study leads to the determination of the critical section of the tree to get diameter

• Distribution twisting moment

The torque is distributed on the AD tree whose value is given by the equation 16:

$$T = C_{max} = 10,04 \text{ N.m} \quad (16)$$

Hence the diagram of torque (figure 9):

• Distribution of the bending moment:

• On the plane (A, x, y):

Plotting diagrams of shear forces and bending moment has been done on the software RDM6 and here are the data provided and the results obtained (table 4, 5, 6 and 7):

• Data

- Tables 4 Data provided (A, x, y)

RESULTS

Tableau 5- Données obtenus (A,x,y)

Maximum bending moment = 7424,40 N.m to 80,000 m

- The figure 10, 11, 12 et 13 gives cutting efforts T_z and bending moment T_y respectively
- On the plane (A, x, z):

Data

DataTable 6-provided data (A, x, z)

Results

Table 7- obtained data

- diagram of cutting efforts T_z :
- Bending moment M_y

The analysis of these diagrams shows that the critical section at C:

$$M_C = \sqrt{M_{CZ}^2 + M_{CY}^2} = \sqrt{(-49610,4)^2 + (7424,40)^2} \Rightarrow M_C = 50,2 \text{ N.m} \quad (16)$$

- The torque is:

$$T_C = 10,04 \text{ N.m} \quad (17)$$

- The axial force at C:

$$F_C = X_B = 0 \text{ N} \quad (18)$$

Code ASME (American Society of Mechanical Engineers)

a)ASME code (American Society of Mechanical Engineers)

The method of the ASME code is a tool very useful in the design, because it allows to quickly evaluating the diameter of a tree, sollicited to both torsional and bending, using theory a static limitation based off on the maximum shear stress (Drouin, 2011). ASME sets the maximum allowable stress $[\sigma]$ as the smaller of the two values of the equation 19

$$[\sigma] = b * (0.18 * R; 0.3 * Re) \text{ min} \quad (19)$$

Or: R_e is the yield stress and

$$b = \begin{cases} 1,0 & \text{without stress concentration.} \\ 0,75 & \text{with stress concentration} \end{cases}$$

The calculation of the maximum shear stress based on the Mohr circle is given with formula 20:

$$\tau = \frac{16}{\pi \cdot d^3} \left(\sqrt{((Cm \cdot M)^2) + (Ct \cdot T)^2} \right) \quad (20)$$

Equations (18) and (19) are combined to give:

$$d = \left[\frac{5,1}{[\sigma]} * \left((Cm * M)^2 + (Ct * T)^2 \right)^{\frac{1}{2}} \right]^{1/3} \quad (21)$$

Ct and Cm are load factors [7]

Next conditions for tree services, the materials should have enough high strength characteristics. The determination of the diameter depends on mechanical properties of the shaft material. Five materials were chosen (Steel S 235, Steel S 335, 42 CD 4, 34 Cr Mo 4 and 36 Ni Cr Mo 16) and diameters corresponding were evaluated in Table 8. Figure 14 shows the evolution of the shaft diameter depending on selected materials and it also shows that when the yield stress increases the value of impoverished diameter. Similarly, when the allowable stress of the ASME code is the value of maximum diameter corresponds is minimal. The calculated diameters must undergo a verification calculation, firstly, to validate the calculated dimensions and check the resistance mechanical of the type of material chosen and ensure that it can withstand the conditions.

Verification and final choice of shaft diameter: The main aim is to make optimal choice of the diameter of the tree while validating its mechanical strength. According to (Jong Boon Ooi1 – Xin Wang, 2013) two methods exist the first is experimental by performing mechanical testing and the second is the Finite Element Analysis (FEA). The AEF is a numerical method widely accepted in the evaluation and verification of tree design (Opalić, 2011). Recently, (Ooi, 2012) analyzed contact stress gearing in a gearbox using AEF. (Göksenli, 2009) Used AEF to simulate stress analysis on the shaft keying a lift to validate their mathematical model to determine the maximum stress. (Bayrakceken, 2007) Determine the conditions stress distributions on a gimbal's shaft section using the FEA method.

Finite Element Analysis (FEA): FEA is a method for performing numerical simulations of physical phenomena. It consist to determine constraints at any point of the geometric model, deformations and displacements under the action of the factor of external forces while checking its mechanical strength. The criteria used in this study is that of Von Mises.

Von Mises strength criterion: The strength criterion adopted for this study is the criterion of Von Mises. Indeed, every element of the structure must verify that the equivalent von Mises stress is less than the allowable stress of the material.

$$\sigma_{\text{eq}} \leq \sigma_{\text{adm}} \tag{22}$$

The equivalent von Mises stress is::

$$\sigma_{\text{eq}} = \sqrt{\sigma_x^2 + \sigma_y^2 + \sigma_z^2 - \sigma_x \sigma_y - \sigma_x \sigma_z - \sigma_y \sigma_z + 3\tau_{xy}^2 + 3\tau_{xz}^2 + 3\tau_{yz}^2}$$

The stress tensor is written:

$$[\sigma] = \begin{bmatrix} \sigma_x & \tau_{xy} & \tau_{xz} \\ \tau_{xy} & \sigma_y & \tau_{yz} \\ \tau_{xz} & \tau_{yz} & \sigma_z \end{bmatrix}$$

The allowable stress is given by the following equation:

$$\sigma_{\text{adm}} = \frac{R_e}{S_e} \tag{23}$$

R_e is the yield strength of the material and S_e is the safety factor, it is chosen from (Drouin, 2011). The model usually includes graphical geometry of the geometric model, with its mesh of finite elements, the definition of material properties, application loading and boundary conditions. The digital simulation software used for the FEA is Catia V5. Each diameter calculated by the ASME code will be checked by the method FEA. Figure 15 describes all the stages of the FEA method. In each case, the equivalent stress von Mises, static deformation in any point of the geometric model will be determined.

Simulation results : Table 9 shows the results of simulations performed under the Catia5 environment. Each diameter is estimated the maximum equivalent von Mises stress and maximum deformation corresponding static. All pre-selected materials satisfy the equivalent Von Mises stress is less than the allowable stress of the material that is to say a good mechanical strength. The diameters of 13, 1 and 7.2 mm 34 Cr Mo 4 and 36 Ni Cr Mo 16 respectively can't withstand the applied stresses, because the tree ruptures during simulation. Three diameter values are favorable, respectively 50; 35 and 25 mm Designers and engineers of trees constantly found ways to optimize sections of trees by adjusting all the parameters to obtain a better ratio strength-weight. Based on this recommendation the diameter of 25 mm of 42 CD 4 material is more competitive than those of 50 and 35 mm whose materials Steel S 235 and S 335, respectively, point of view the resistance of material, 42 CD 4 is two times stronger than steel S 235 and S 335 steel, Also the density of materials is constant, which allows to say that the weight of the diameter of 25 is lower than the others. In conclusion, the diameter 25 mm of the material 42 CD 4 is finally selected for the production of the shaft of the mill.

2.1.The Finite Element Analysis for Diameter 25: The Driveshaft chose is of 42 CD 4 whose mechanical characteristics are presented in Table 9 Table 10-mechanical characteristics of the steel 42CD4

•loadings applied to the shaft are listed in Table 11:

Figure 16 shows the geometrical model of the driven shaft of the machine.

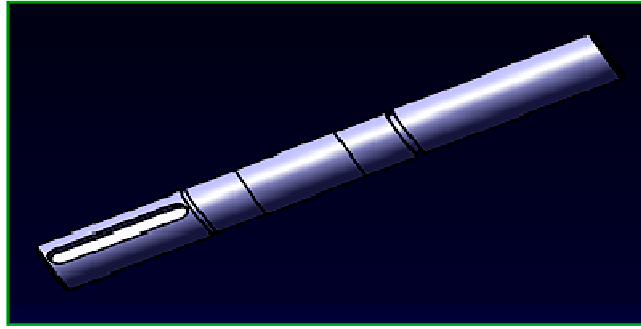


Figure 16. Geometric tree Model

Figure 17 shows the boundary condition and load applied to the shaft

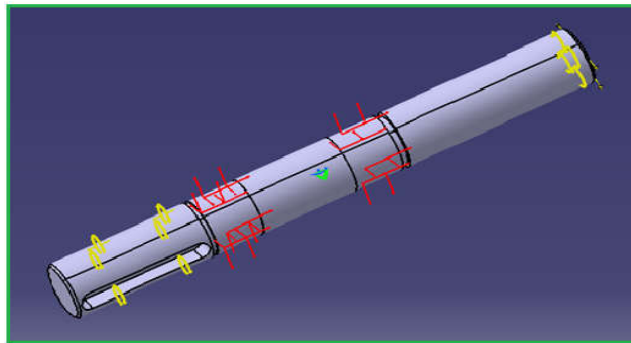


Figure 17. Boundary condition and load applied to the shaft

Figure 18- shows the deformed and the finite element model of the output shaft.

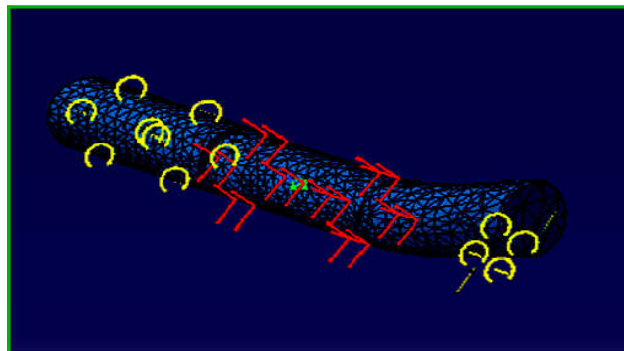


Figure 18. Distorted and finite element model of the tree

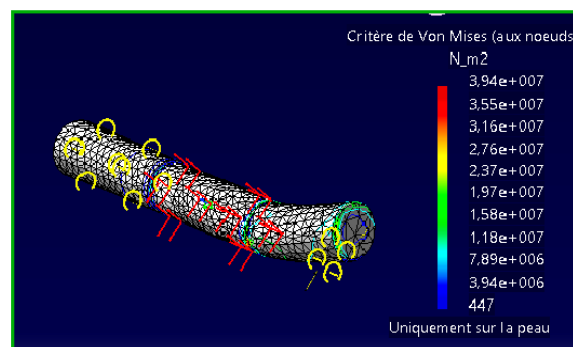


Figure 19. Distribution of the von Mises

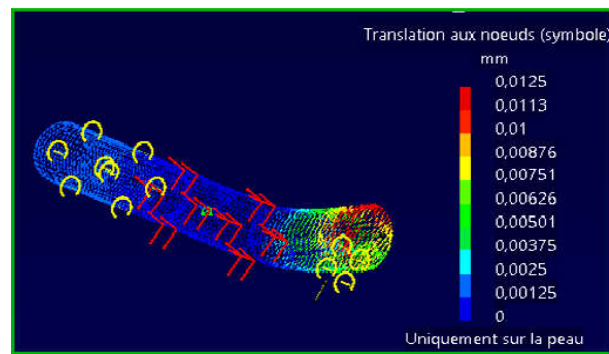


Figure 20. Distribution of the static deformation

The mesh has the following characteristics

- Quality of the mesh: Medium
- Total number of nodes: 10285
- Total items: 5976
- Number of D.D.L: 30855

The Von Mises stress distribution is shown in Figure 19. The allowable stress is $\sigma_{adm} = 233.33 \text{ MPa}$ indeed $S_e = 3$ and $R_e = 700 \text{ MPa}$. Note that the maximum von Mises stress is about 39.4 MPa, which is well below the allowable stress. Figure 20- shows the distribution of the static deformation at the tree. It is found that the maximum value of the deformation is in the range of 1.25 E^{-02} .

Conclusion

The objective of this research is to design, modeled, dimensioned and analyzes the behavior of a power transmission shaft of a solar hammer mill. The tree model was designed and sized by analytical and empirical equations such as the ASME code. It has been validated and optimized by the method of the FEA. The evaluation of various types of materials for choosing optimal diameter enables weight saving of 40% to 70%. Simulation results by the AEF show that the maximum equivalent von Mises stress for the selected final diameter is about 39.4 MPa which is well below the allowable stress, previously defined as the ratio of the limit elasticity of the material $R_e = 700 \text{ MPa}$ and a safety factor set at $S_e = 3$. The maximum value of the static deformation is of the order of $1.25 \text{ E}^{-02} \text{ mm}$ lower 3 mm, the game allowed between the screen and the hammer. Static study shows that the calculated and chosen dimensions (25mm in diameter and 200mm in length) are acceptable for the particular case of operation.

REFERNCES

- Gueye, A.1996. «*Conception d'une machine manuelle à décortiquer et à moudre le mil*». Thiès: Ecole polytechnique de .
- Bayrakceken, H. T. 2007. Two cases of failure in the power transmission system on vehicles: A universal joint yoke and a drive shaft. *Engineering Failure Analysis*,.
- Drouin, G. 2011. *Eléments de machines-deuxième édition*.
- Göksenli, A. E. 2009. Failure analysis of an elevator drive shaft. *Engineering FailureAnalysis*,.
- GTZ. Février 2004. «*Promotion de l'Electrification Rurale et de l'Approvisionnement Durable en Combustibles Domestiques PERACOD*» ; les applications photovoltaïques génératrice de revenus. Dakar.
- Jong Boon Ooi1 – Xin Wang, Y. P. 2013. Parametric Optimization of the Output Shaft of a Portal Axle using Finite Element Analysis. *Journal of Mechanical Engineering*.
- Ooi, J. W. 2012. Modal and stress analysis of gear traindesign in portal axle using finite element modelingand simulation. *Journal of Mechanical Science andTechnology*.
- Opalić, M. K. 2011. Proofof strength of shafts and axles using finite elementmethod. *FAMENA*.
- Ranganath, V. D. 2004. Failure of a swing pinion shaft of a dragline.
- Shigley, J. M. 1989. Mechanical Engineering Design. *McGraw Hill Publication*.
- Spotts, M. 1991. Design of Machine Elements. *Prentice Hall India*.
- Standard, A. 1985. Design of Transmission Shafting. *American Society of Mechanical Engineers*, 106.
